SUPPLEMENTARY INFORMATION: Efficiency enhancement of small molecule organic solar cells using hexapropyltruxene as an interface layer

Hanyang Ye,*[a] Sameer Vajjala Kesava,[a] Josue Martinez Hardigree,[a] Roisin E. Brown,[b] Giulio Mazzotta,[a] Ross Warren,[a] Peter J. Skabara,[b‡] and Moritz Riede*[a]

* Corresponding authors
[a] Clarendon Laboratory, Parks Road, Oxford OX1 3PU, England, UK. Tel: +44-18 6528 2328; E-mail: hanyang.ye@physics.ox.ac.uk & moritz.riede@physics.ox.ac.uk
[b] WestCHEM, Department of Pure and Applied Chemistry, University of Strathclyde, Glasgow, G1 1XL, UK.
‡ Present address: School of Chemistry, Joseph Black Building. University Avenue, Glasgow, G12 8QQ, UK.

1 UV-vis, XRD, and AFM measurements of 100 nm hexapropyltruxene layer

Measurements of the UV-vis spectra of 100 nm hexapropyltruxene layer made in VC-A show that this thin film is almost transparent in the visible spectrum region, which is desired for being an interlayer in a solar cell stack (Figure S1). A Tauc Plot analysis suggests its optical band gap is 3.9 eV. Cyclic Voltammetry measurement shows the hexapropyltruxene has reversible oxidation, but no reduction is observed in the scanned range from 1.75 to 5 V. The value used for Eox vs Li/Li^+ is 4.39 V. The HOMO is subsequently calculated as -5.53 eV (Figure S2). XRD and AFM analysis of the identical hexapropyltruxene layer (100 nm) show that it is an X-ray amorphous thin film with a surface roughness of 0.4 nm. (Figure S3 & Figure S4).

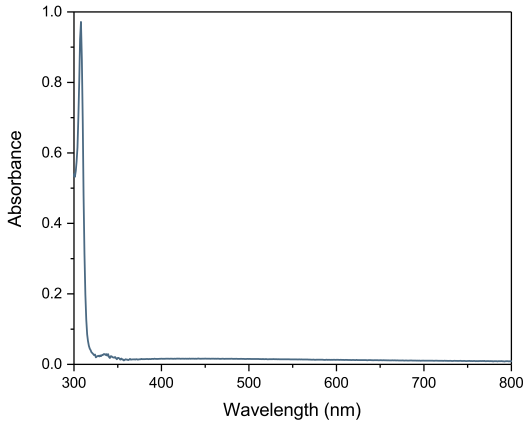

Figure S 1. UV-vis spectrum of 100 nm hexapropyltruxene layer.

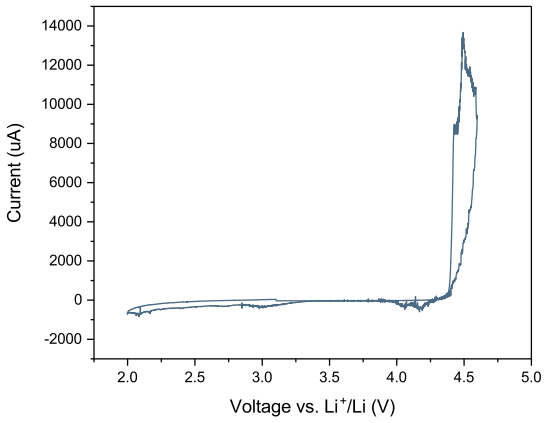

Figure S 2. Cyclic voltammetry test result of hexapropyltruxene.

2 AFM Analysis of the in-situ GIWAXS samples

To further confirm the morphology change of SubPc on substrates and hexapropyltruxene, AFM measurement of SubPc layer on different substrates (made in VC-C) were carried out. Figure S5(a) and (b) show the surface topography of 13 nm SubPc on Si wafer. It has a roughness (RMS) of 0.50 nm, Figure S5(c) and (d) show the surface morphology of 13 nm SubPc on 3.8 nm hexapropyltruxene deposited on Si wafer. The roughness we obtained is 0.64 nm. Figure S5(e) and (f) show the morphology of 13 nm SubPc on ITO glass and 5 nm

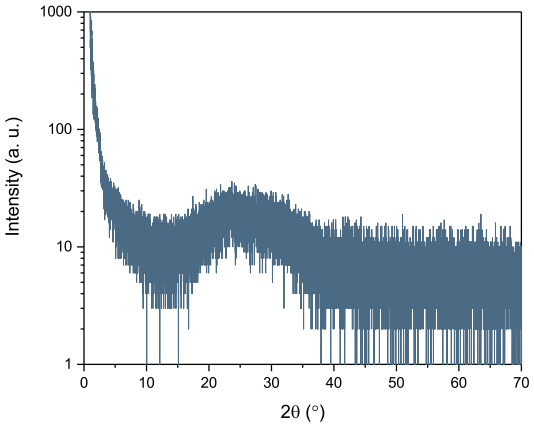

Figure S 3. XRD analysis of 100 nm hexapropyltruxene layer on glass substrate.

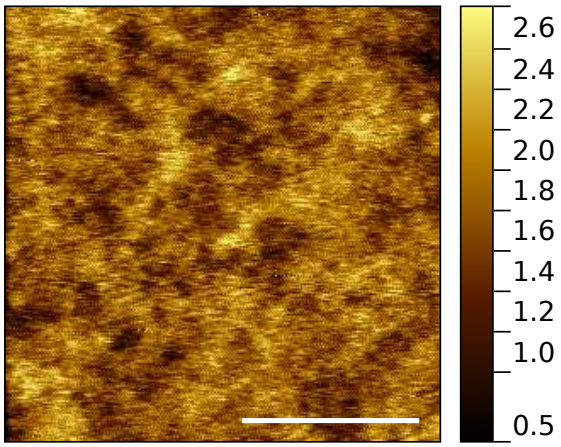

Figure S 4. AFM image of the surface morphology of hexapropyltruxene layer (100 nm). The scale bar in the figure is 2 μm and the unit for the vertical scale is nm.

MoO_x, the roughness is 0.45 nm, Figure S5(g) and (h) show the morphology of 13 nm SubPc on 3.8 nm hexapropyltruxene deposited on ITO glass and 5 nm MoO_x, the roughness is 0.55 nm. From the AFM analysis, we can conclude that both on Si and ITO/MoO_x film, SubPc appears to have a slightly rougher surface morphology if there is a hexapropyltruxene interlayer. Also, from the AFM images, we can see that the feature size of SubPc becomes smaller after inserting the hexapropyltruxene layer. We used the segmentation function in gwiddeon to calculate the 'grain size' of the surface. However, this 'grain' concept is just

a model concept, and by comparing this parameter between the samples, we can have an imagistic knowledge about the surface shape and roughness. The calculated mean 'grain size' shrinks from 54 nm to 36 nm after inserting the hexapropyltruxene layer. This evidence shows that hexapropyltruxene interlayer does modify the morphology of SubPc layer on top of it.

3 Ellipsometry simulation

The refractive indices (n, k) of hexapropyltruxene is plotted in Figure S6. We used the refractive indices data of materials to simulate the transmittance and reflectance of the multilayer stack to confirm the accuracy of our ellipsometry model. The result is shown in Figure S7, indicating a good agreement between our model and the experimental data. We used these refractive indices values to simulate the absorption of our solar cell stacks with and without hexapropyltruxene (see in Figure S9). The dips just before the onset of the absorption of the SubPc layer in the stack with hexapropyltruxene is due to the different refractive indices of the MoO_x layer and the additional layer of hexapropyltruxene.

4 Solar Cell Mismatch Factor Calculation

We have calculated the mismatch factor for the reference solar cell without hexapropyltruxene, and the solar cell with hexapropyltruxene was calculated as 0.98(0) and 0.97(7), respectively, which is close to unity. The spectra of solar simulator lamp, AM 1.5G, as well as EQE comparison of the standard reference, SubPc/C60 solar cell without hexapropyltruxene (i.e. reference solar cell in the manuscript), and SubPc/C60 solar cell with 3.8 nm hexapropyltruxene are shown in Figure S8.

5 Stack absorption simulation

Table S 1. Photon number absorbed in each layer calculated by absorption simulation using a transfer matrix approach.

Device	Absorbed photon number ($\times 10^{16}$)			Absorbed photon percentage (%)	
	SubPc	C60	Total	SubPc	C60
Reference device	3.28	2.78	9.19	36	30
Device with 3.8 nm hexapropyltruxene	2.90	2.97	9.05	32	33

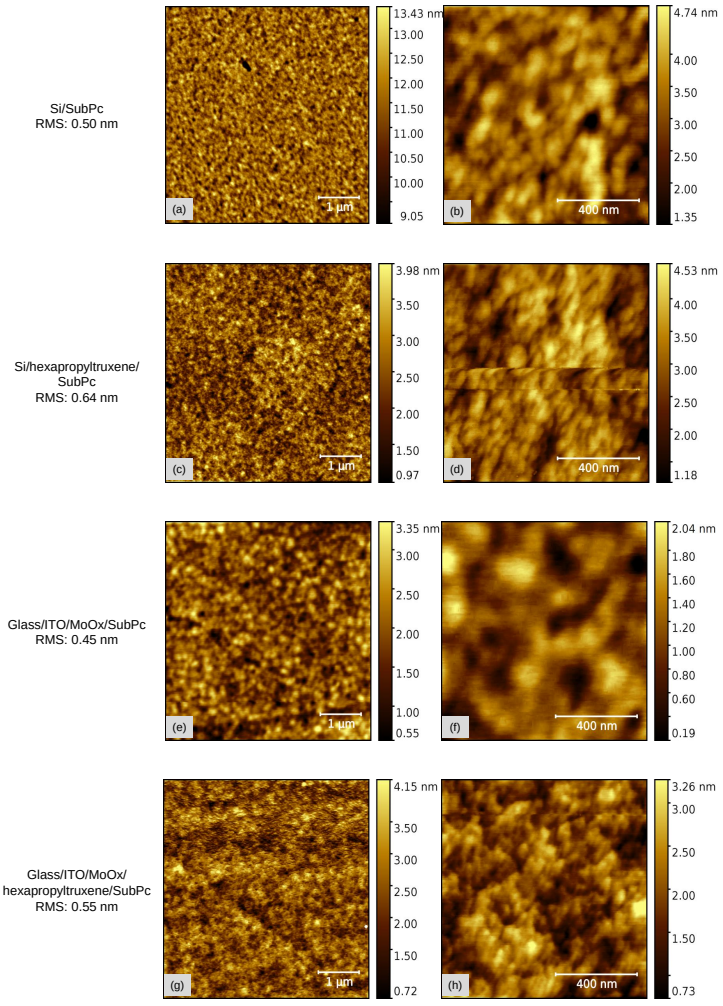

Figure S 5. AFM images of the surface morphology of 13 nm SubPc deposited on different layers with the left column being 5x5 μm^2 and the right column a zoomed-in version of 1x1 μm^2: (a) & (b): Images of SubPc layer on a Si wafer. (c) & (d): images of Si/hexapropyltruxene (3.8 nm)/SubPc multilayer film. (e) & (f): Images of ITO/MoO_x(5 nm)/SubPc multilayer film. (g) & (h): Images of ITO/MoO_x(5 nm)/hexapropyltruxene(3.8 nm)/SubPc multilayer film.

6 IQE Measurement

We further calculated the IQE using the EQE and UV-vis reflectance data to compare the charge generation in the devices. Shown in Figure S10 are the

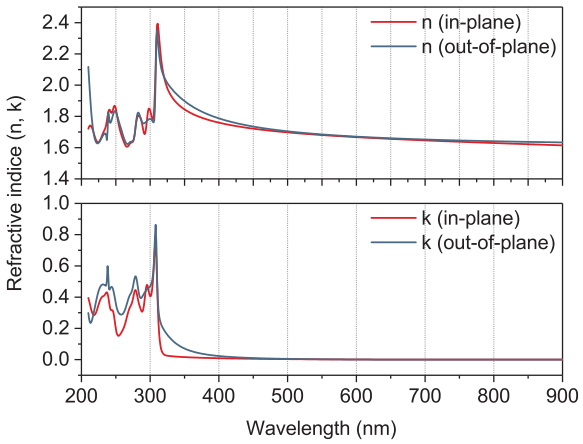

Figure S 6. Refractive indices n, k (in-plane and out-of-plane) of hexapropyltruxene determined form a Si/hexapropyltruxene (28 nm) sample.

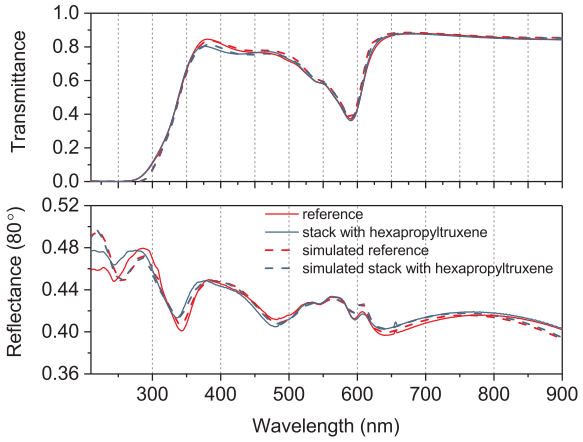

Figure S 7. Reflectance (measured at incidence angle=80°) and transmittance (incidence angle=0°) of reference film (glass/ITO/ SubPc (13 nm)) and film with hexapropyltruxene (glass/ITO/MoO_x (5 nm)/SubPc (13 nm)). The solid lines are reflectance measured, the dashed lines are the data simulated with the ellipsometry data.

results: with the insertion of hexapropyltruxene layer, IQE increases significantly within the wavelength range of 475 nm to 600 nm, which is the main absorption range of the device and the SubPc absorption region. Calculated photocurrent generation increase is 39 % comparing with the reference device.

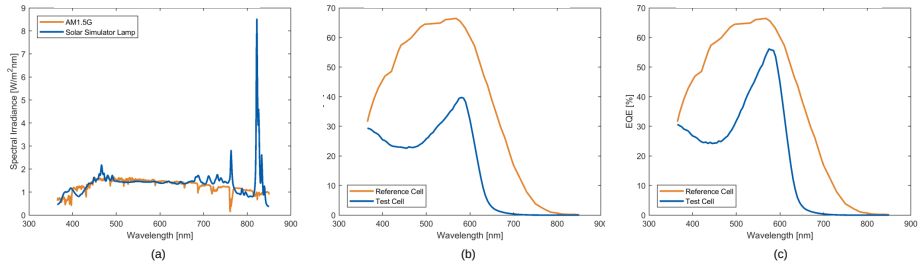

Figure S 8. Solar cell mismatch factor calculation result. (a). the spectra of solar simulator lamp and AM 1.5G, (b). EQE comparison of the standard reference and SubPc/C60 solar cell without hexapropyltruxene (i.e. reference solar cell in the manuscript), (c). EQE comparison of the standard reference and SubPc/C60 solar cell with 3.8 nm hexapropyltruxene.

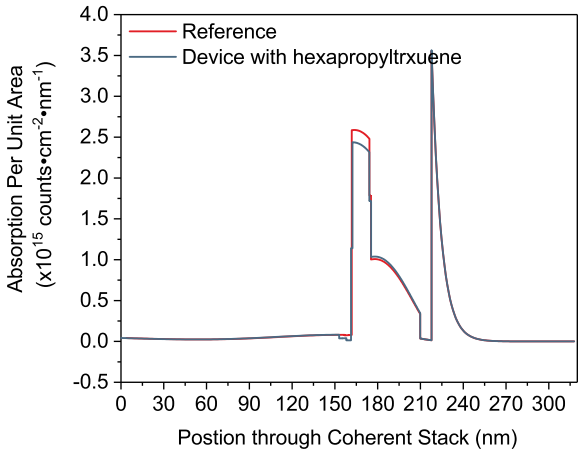

Figure S 9. Absorption simulation of solar cell stack with/without hexapropyltruxene using a transfer matrix approach.

This result shows that the inserted hexapropyltruxene helps to turn more of the photogenerated excitons in the SubPc into current that can be extracted.

7 Solar Cell Performance Summary

The device performance summary of solar cells with different thicknesses of hexapropyltruxene is shown in Table S2.

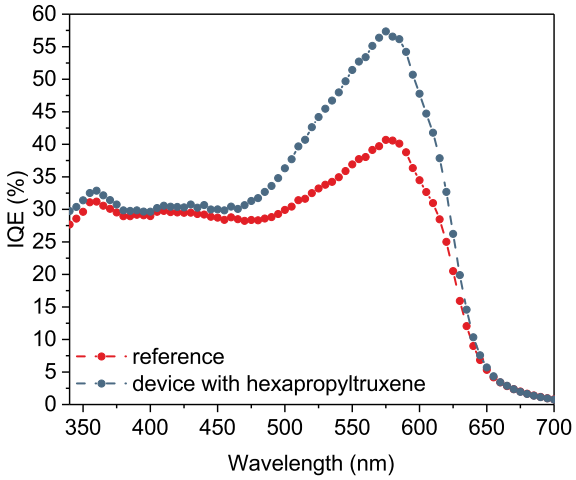

Figure S 10. Internal quantum efficiency (IQE) calculations based on the EQE and absorption data (see Fig. 4) for the reference devices without hexapropyltruxene and the devices with 3.8 nm hexapropyltruxene as interlayer between MoO_x and SubPc (stack see Fig. 1a).

Table S 2. Device performance summary of solar cells with different thicknesses of hexapropyltruxene.

Hexapropyltruxene thickness (nm)	J_{sc}(mA·cm^{-2})	V_{oc} (V)	FF (%)	PCE (%)
0	4.1 ± 0.06	1.10 ± 0.01	56 ± 1	2.6 ± 0.03
0.8	4.5 ± 0.15	1.11 ± 0.01	55 ± 1	2.7 ± 0.05
2.3	4.9 ± 0.09	1.11 ± 0.01	55 ± 1	3.0 ± 0.09
3.8	5.1 ± 0.04	1.11 ± 0.01	53 ± 1	3.0 ± 0.08
5.4	4.8 ± 0.11	1.12 ± 0.01	42 ± 1	2.3 ± 0.13
7.7	4.7 ± 0.04	1.12 ± 0.02	28 ± 2	1.5 ± 0.11